Water Adsorption on AnO_2 (111), (110) and (100) Surfaces (An = U, Pu); A Computational Study

Bengt E. Tegner*[1], Marco Molinari[2], Andrew Kerridge[3], Stephen C. Parker[2], and Nikolas Kaltsoyannis*[1]

[1] School of Chemistry, The University of Manchester,

Oxford Road, Manchester, M13 9PL, UK.

[2]Department of Chemistry, University of Bath,

Claverton Down, Bath, BA2 7AY, UK.

[3] Department of Chemistry, Lancaster University,

Bailrigg, Lancaster, LA1 4YW, UK.

*Correspondence: bengt.tegner@manchester.ac.uk, nikolas.kaltsoyannis@manchester.ac.uk

Abstract

The interactions between water and the actinide oxides UO_2 and PuO_2 are important when considering the long-term storage of spent nuclear fuel. However, experimental studies in this area are severely limited by plutonium's intense radioactivity, and hence we have recently begun to investigate these interactions computationally. In this article we report the results of plane-wave density functional theory calculations of the interaction of water with the (111), (110) and (100) surfaces of UO_2 and PuO_2, using a Hubbard-corrected potential (PBE+*U*) approach to account for the strongly-correlated 5f electrons. We find a mix of molecular and dissociative adsorption to be most stable on the (111) surface, and that fully dissociative adsorption is the most stable configuration on the (110) and (100) surfaces, leading to a fully hydroxylated monolayer. From these results we derive water desorption temperatures at various pressures for the different surfaces.

Introduction

The reprocessing of UO_2-based spent nuclear fuel in the UK has led to the accumulation, over several decades, of significant quantities of highly radioactive PuO_2. Indeed, the UK holds about half the world's civil inventory of PuO_2 (126 tonnes Pu) [1], stored as a powder in stainless steel containers, while the government decides its long term fate. Options include long term storage in a geological disposal facility, or reuse in mixed oxide fuel, but for the time being the policy is interim storage pending a final decision. However, some of these steel containers have buckled, leading to the hypothesis that gas build up has occurred, possibly from water vapor due to desorption from the PuO_2, the production of hydrogen gas due to the radiolysis of water, or chemical reaction of water with PuO_2. It is essential that we fully understand the causes of the container distortions, and hence we are exploring these suggestions computationally. In this contribution we report our investigations of water adsorption on the low index surfaces of UO_2 and PuO_2, as well as comparing our results with previous work reported in the literature.

Experimental work in this area, especially featuring PuO_2, is very challenging. One of the first mentions of water interactions with PuO_2 was by Haschke *et al*. [2], who suggested that water/PuO_2 interaction led to the formation of the higher oxide PuO_{2+x}. They proposed that water adsorbs in stages, with a first layer of strongly bound, chemisorbed water producing a hydroxylated

surface due to dissociation followed by one or more weakly bound layers of molecular water. Earlier, Stakebake [3] measured water desorption temperatures on PuO_2 and reported water desorbing in two distinct temperature ranges, one at 373 - 423 K and another at 573 - 623 K, also suggesting a strongly bound first layer followed by a more weakly bound second layer; he estimated a desorption energy of -2.94 eV for this first layer. Paffet *et al.* [4] confirmed this process and revised the adsorption energy of the first layer to -1.82 eV, and suggested -1.11 eV for the second layer at 371 K.

Previous theoretical investigations have focused mainly on UO_2, and have disagreed as to whether molecular or dissociative adsorption is the more favorable on the (111) surface. Skomurski *et al.* [5] and, more recently, Weck *et al.* [6] found molecular adsorption to be the more favorable on this surface, with adsorption energies of -0.69 eV and -0.77 eV per water molecule respectively, using periodic density functional theory (DFT) with the generalized gradient approximation (GGA) of Perdew and Wang (PW91) used for the exchange-correlation energy. Tian *et al.* [7] also found molecular adsorption to be the stronger on UO_2 (111), with an adsorption energy of -1.08 eV. These workers employed DFT+*U* [8], [9], a method which addresses the failure of standard DFT to correctly describe the insulating behavior of the actinide dioxides by introducing a Hubbard *U* term to better describe the strongly correlated 5f electrons. By contrast, Bo *et al.* [10], also using DFT+*U*, found that a mixed molecular and dissociative configuration is the

Commented [A1]: Is this correct? It's the approximate functionals which cause the problem, not DFT itself

most stable on UO_2 (111), with an adsorption energy of -0.65 eV. These workers also studied water adsorption on the UO_2 (110) and (100) surfaces, finding dissociative adsorption to be the more favorable on both surfaces, with energies of -0.93 and -0.99 eV respectively.

Theoretical studies of water adsorption on PuO_2 are less numerous. Wu *et al.* [11] studied water on the PuO_2 (110) surface using the local density approximation (LDA) and found dissociative adsorption to be favorable with an adsorption energy of -0.49 eV. More recently, Jomard *et al.* [12] also found dissociative adsorption to be the more favorable on the PuO_2 (110) surface with an adsorption energy of -0.95 eV using the PBE+*U* approach. Moreover, Rák *et al.* [13] found that hydroxylation of the AnO_2 (111), (110) and (100) surfaces stabilizes the wet (110) and (100) surfaces compared with the wet (111), reversing the trend found for dry surfaces.

We have very recently reported a theoretical study of molecular and dissociative water adsorptions on the (111) and (110) surfaces of both UO_2 and PuO_2, using hybrid DFT (PBE0) within an embedded cluster framework [14]. Adsorptions on the (110) surface are stronger than on the (111). Similar energies are found for molecular and dissociative adsorption on the (111) surfaces, while on the (110) there is a clear preference for dissociative adsorption, as emerges from the periodic DFT studies discussed above, and also in agreement with the experimental suggestions of a fully hydroxylated first layer.

The present paper is organized as follows: we start with a brief description of the computational methodology used, followed by the results for the dry surfaces. We then discuss water adsorption geometries and energies on the (111), (110) and (100) surfaces, comparing molecular and dissociative adsorption at various coverages, and finish with predictions of water desorption temperatures over a wide range of pressures. Throughout, we compare our data with previous theoretical and, where possible, experimental results.

Methodology

All calculations were performed using VASP 5.4.1 [15], a plane-wave DFT code using Projector-Augmented Wave (PAW)-pseudopotentials [16] to describe the ions and employing Monkhorst-Pack (MP) [17] grids for the *k*-space integration. All calculations used a plane wave cut-off of 650 eV and a minimum MP-grid of 5×5×1 *k*-points for the Brillouin zone sampling. The generalized gradient approximation of Perdew, Burke, and Ernzerhof (PBE) [18], with a Hubbard *U* correction for the 5f electrons [8], [9], was used for the exchange-correlation energy.

The AnO_2 surfaces are constructed using repeating slabs of 16 AnO_2 units arranged in four layers for the (111) surface and 24 AnO_2 units arranged in six layers for the (110) and (100) surfaces, each with 18 Å of vacuum between each slab. The entire system is allowed to relax until the inter-atomic forces are below 0.001 eV/Å. We use **1-k** co-linear magnetic ordering with net magnetic moment of zero, allowing us to treat the total system as anti-ferromagnetic and thereby reach the correct ground state [19], [20]. We neglect spin-orbit coupling, as earlier results by Rák and co-workers [13] indicate that spin-orbit coupling ~~only~~ has only a very small effect on the surface stability.

The adsorption energy per water molecule is given by the following expression:

$$E_{ads} = \left[E_{(slab+mol)} - (E_{slab} + n_{mol} \times E_{mol})\right]/n_{mol}$$

where $E_{(slab+mol)}$ and E_{slab} are the energies of the slab with the adsorbed molecule and the clean slab, respectively, and E_{mol} is the energy of a water molecule in the gas phase, calculated in VASP using a single water molecule in a large box with a 20 Å side.

Due to the very large number of possible adsorption configurations, we have focused on a small number of likely minimum-energy initial geometries, based on maximizing hydrogen bonding between the adsorbate and the surface at low coverage, and the most stable configuration was kept up to full coverage. Adsorbates are introduced on both sides of the slab to minimize dipole effects, as used by Molinari and co-workers [21].

Dependence on the effective *U* parameter

Previous work has indicated the necessity of using the GGA+*U* formalism [8], [9] to correctly describe the AnO_2 surfaces [13], [22]. To verify the dependence on the effective *U* parameter, U_{eff} = (*U*-*J*), we calculated the adsorption energy of a single water molecule on the (111) surface for U_{eff} ranging from 3 - 5 eV for UO_2 and 4 - 7 eV for PuO_2. We found an energy difference of only 0.05 eV between these extremes, in good agreement with previous work by Weck and colleagues [6], who also found a weak dependence on *U*. In light of this and other studies, using Dudarev's formalism [8] we choose an effective U_{eff} = 4 eV for both UO_2 and PuO_2, as employed previously in the literature.

Results and Discussion

Dry Surfaces

Bulk UO_2 and PuO_2 adopt the fluorite structure [23]. We started by constructing our three target low index surfaces by cleaving the bulk along the oxygen-terminated (111), (110) and (100) planes. The (100) surface was modified by moving half of the oxygens from the bottom to the top, creating a slab without a dipole moment. During relaxation, the An-O bond distances in the outermost layers on the (111), (110), and (100) surfaces decrease by about 0.02 Å compared with the bulk.

The calculated surface energies are 0.65, 1.05, and 1.33 J/m for the UO_2 (111), (110), and (100) surfaces, and 0.66, 1.13, and 1.59 J/m for the analogous PuO_2 surfaces. This sequence is consistent with other oxide surfaces with the fluorite structure, and the calculated surface energies compare well with previous work by Rák *et al.* [13].

Adsorption on the AnO_2 (111) surface

A ball-and-stick representation of a single water molecule adsorbing molecularly on the (111) surface supercell is shown in figure 1, and the calculated adsorption energies of molecularly and dissociatively adsorbed water on UO_2 (111) and PuO_2 (111) are collected in tables 1 and 2. Data from earlier studies on UO_2 from Bo and co-workers [10] as well as Tian and colleagues [7], plus UO_2 and PuO_2 from Rák and colleagues [13], and recent

work from our group [14] are shown for comparison. Corresponding data on CeO_2 (111) from Molinari and co-workers [21] are shown in table 3 and selected inter-atomic distances for water on all three metal oxide (111) surfaces are given in table 4.

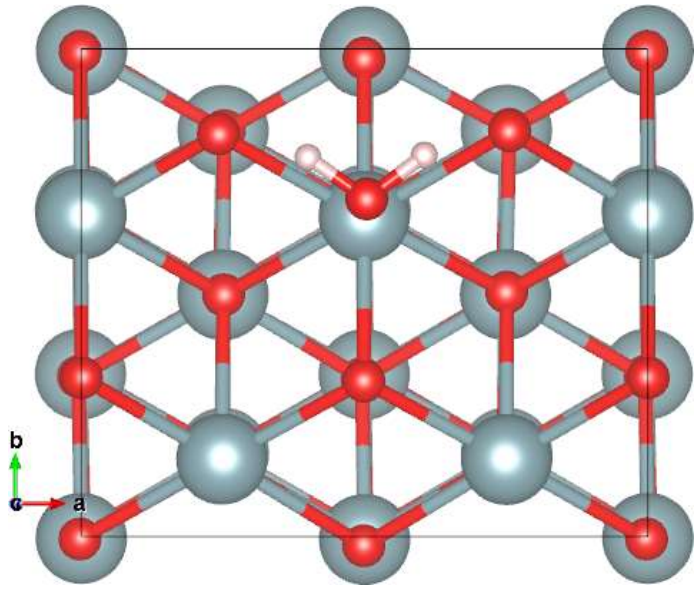

Figure 1: Single water molecule adsorbed molecularly on the 2 × 2 UO_2 (111) surface, yielding a coverage of 25%, i.e. ¼ of a mono-layer. U atoms in gray, oxygen in red and hydrogen in white.

System	UO_2 (111) + 1 × H_2O	UO_2 (111) + 2 × H_2O	UO_2 (111) + 3 × H_2O	UO_2 (111) + 4 × H_2O
H_2O adsorption	-0.53	-0.53	-0.53	-0.49
OH + H adsorption	-0.50	-0.41	-0.29	-0.15
H_2O adsorption [14]	-0.52	N/A	-0.64	N/A
OH + H adsorption [14]	-0.63	-0.56	-0.53	N/A
H_2O adsorption [10]	-0.61	N/A	N/A	-0.60
OH + H adsorption [10]	-0.68	N/A	N/A	-0.32
H_2O adsorption [7]	-1.08	N/A	N/A	N/A
OH + H adsorption [7]	-0.68	N/A	N/A	N/A
OH + H adsorption [13]	N/A	N/A	N/A	-0.29

Table 1: Adsorption energies in eV per water molecule on UO_2 (111).

System	PuO_2 (111) + 1 × H_2O	PuO_2 (111) + 2 × H_2O	PuO_2 (111) + 3 × H_2O	PuO_2 (111) + 4 × H_2O
H_2O adsorption	-0.40	-0.47	-0.46	-0.44
OH + H adsorption	-0.32	-0.29	-0.21	-0.07
H_2O adsorption [14]	-0.53	-0.52	-0.53	-0.59
OH + H adsorption [14]	-0.45	-0.39	-0.42	-0.32
OH + H adsorption [13]	N/A	N/A	N/A	-0.23

Table 2: Adsorption energies in eV per water molecule on PuO_2 (111).

System	CeO_2 (111) + 1 × H_2O	CeO_2 (111) + 2 × H_2O	CeO_2 (111) + 4 × H_2O
H_2O adsorption [21]	−0.56	−0.60	−0.57
OH + H adsorption [21]	−0.59	N/A	−0.15

Table 3: Adsorption energies in eV per water molecule on CeO_2 (111).

Distance (Å)	UO_2 (111) + 0.25 - 1.0 ML	UO_2 (111) + 0.25 - 1.0 ML [10]	PuO_2 (111) + 0.25 - 1.0 ML	CeO_2 (111) + 0.25 - 1.0 ML [21]
H_W – O_S	1.96 - 2.28	1.66	2.00 - 2.23	1.99 – 2.13
An_S/Ce_S - H_2O	2.62 - 2.68	2.60 - 2.73	2.62 - 2.68	2.62
An_S/Ce_S – O_WH_W	2.18 - 2.26	2.29 - 2.36	2.20 - 2.26	2.22
An_S/Ce_S – O_SH_W	2.33 - 2.44	N/A	2.30 - 2.43	2.41
O_SH_W – O_WH_W	1.61 - 2.39	N/A	1.56 - 2.29	1.65

Table 4: Selected inter-atomic distances for molecularly and dissociatively adsorbed water on the UO_2 (111) and PuO_2 (111) surfaces at coverages from 0.25 to 1.0 mono-layers, with results for UO_2 from Bo *et al.* [10] and for CeO_2 from Molinari *et al.* [21]. H_W and O_W denote the hydrogen and oxygen atoms belonging to the water molecule whereas An_S/Ce_S and O_S denote the outermost surface atoms. O_WH_W denotes the hydroxyl molecule made from the dissociated water molecule and O_SH_W denotes the other hydroxyl molecule made from a surface oxygen and the remaining hydrogen.

Commented [A2]: This seems rather awkward notations. Couldn't me just use M to represent the metal ion?

Comparing the adsorption energies for the (111) surface in tables 1 and 2, we find a slight preference for molecular adsorption at low coverage, increasing with coverage to a marked preference at full coverage, with

somewhat lower adsorption energies on PuO_2 compared with UO_2, in good agreement with work by Wellington *et al.* [14]. We interpret this drop in adsorption energy for the dissociative case to weaker hydrogen bonding on the fully hydroxylated surface. We find good agreement between CeO_2 and UO_2/PuO_2 data, particularly at full coverage, strengthening the idea that CeO_2 can be used as a non-radioactive analog of the actinide oxides for experimental water adsorption studies.

Examining the interatomic distances in table 4, we find similar hydrogen bond lengths H_W – O_S in UO_2, PuO_2, and CeO_2, suggesting similar bonding. We also find similar actinide –water distances An_S -H_2O for the three oxides, suggesting similar molecular adsorption geometries. Moreover, the actinide-hydroxyl distances An_S – O_WH_W are shorter than the An_S -H_2O distances, suggesting the hydroxyls sit closer to the surface than the molecular water. Furthermore, the hydroxyl-hydroxyl distances O_SH_W – O_WH_W increase with coverage, suggesting weaker intra-molecular hydrogen bonding for the fully dissociative case.

Commented [A3]: We're doing more than suggesting, aren't we? The data clearly demonstrates this.

We now discuss mixed adsorption at full coverage, going from fully molecular to fully dissociated. The adsorption energies are shown in tables 5 and 6. Corresponding data from Bo and colleagues [10] on UO_2 and from Wellington and co-workers [14] are shown for comparison. We again find close similarity between UO_2 and PuO_2, where the 50/50 mixed case gives the strongest adsorption, in good agreement with Bo's work on UO_2 [10] and recent work by Wellington

Commented [A4]: Wellington et al? I thought coworkers was only used with the senior author, e.g Kaltsoyannis and coworkers.

et al. [14]. Note, however, that the energy difference between the mixed case and the fully molecular one is only 0.07 eV, and the range of adsorption energies is quite compact. We attribute the increased adsorption energy in the mixed case to the formation of stronger intra-molecular hydrogen bonds on the crowded (111) surface compared with the purely molecular case.

System	UO_2 (111) + 4 × H_2O	UO_2 (111) + 3 × H_2O + 1 × (OH + H)	UO_2 (111) + 2 × H_2O + 2 × (OH + H)	UO_2 (111) + 1 × H_2O + 3 × (OH + H)	UO_2 (111) + 4 × (OH + H)
This work	-0.49	-0.51	-0.59	-0.42	-0.15
Wellington *et al.* [14]	N/A	-0.71	-0.74	-0.68	N/A
Bo *et al.* [10]	-0.60	-0.60	-0.65	-0.53	-0.32
Rák *et al.* [13]	N/A	N/A	N/A	N/A	-0.29

Table 5: Adsorption energies in eV per water molecule on UO_2 (111) for mixed molecular and dissociative adsorption.

System	PuO_2 (111) + 4 × H_2O	PuO_2 (111) + 3 × H_2O + 1 × (OH + H)	PuO_2 (111) + 2 × H_2O + 2 × (OH + H)	PuO_2 (111) + 1 × H_2O + 3 × (OH + H)	PuO_2 (111) + 4 × (OH + H)
This work	-0.44	-0.47	-0.50	-0.37	-0.07
Wellington *et al.* [14]	-0.59	-0.55	-0.65	-0.55	-0.32
Rák *et al.* [13]	N/A	N/A	N/A	N/A	-0.23

Table 6: Adsorption energies in eV per water molecule on PuO_2 (111) for mixed molecular and dissociative adsorption.

Adsorption on the AnO_2 (110) surface

The (110) surface is more featured compared with the (111), with alternating rows of oxygens and actinides. A ball-and-stick representation of a single water molecule adsorbing molecularly on the (110) surface at low coverage is

shown in figure 2.

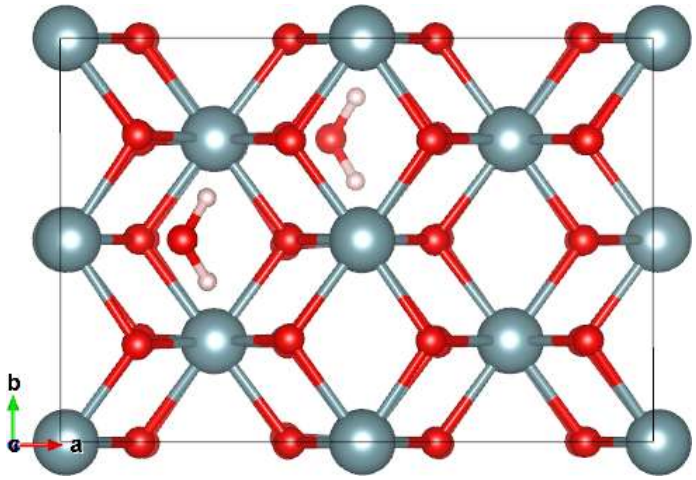

Figure 2: Water adsorbed on the 2 × 2 UO_2 (110) surface, yielding a coverage of 25%, i.e. ¼ of a mono-layer. U atoms in gray, oxygen in red and hydrogen in white. Adsorption occurs on both sides of the slab and, as the two surfaces have equivalent sites that are offset, we can see both the top and the bottom water molecules.

Calculated adsorption energies for molecularly and dissociatively adsorbed water on UO_2 (110) and PuO_2 (110) are collected in tables 7 and 8. Additional data on UO_2 from Bo and co-workers [10], UO_2 and PuO_2 from Rák and colleagues [13] and recent work by Wellington and others [14], plus PuO_2 data from Jomard and colleagues [12], are again shown for comparison. Corresponding data on CeO_2 (110) from Molinari and co-workers [21] are shown in table 9 and selected inter-atomic distances are shown in table 10.

System	UO_2 (110) + 1 × H_2O	UO_2 (110) + 2 × H_2O	UO_2 (110) + 4 × H_2O
H_2O adsorption	-0.93	-0.74	-0.65
OH + H adsorption	-1.39	-1.05	-1.00
H_2O adsorption [14]	-1.06	-0.96	-0.90
OH + H adsorption [14]	-1.60	-1.55	-1.34
H_2O adsorption [10]	-0.62	N/A	-0.62
OH + H adsorption [10]	-1.27	N/A	-0.93
OH + H adsorption [13]	N/A	N/A	-1.05

Table 7: Adsorption energies in eV per water molecule on UO_2 (110).

System	PuO_2 (110) + 1 × H_2O	PuO_2 (110) + 2 × H_2O	PuO_2 (110) + 4 × H_2O
H_2O adsorption	-0.88	-0.73	-0.39
OH + H adsorption	-1.14	-0.94	-0.91
H_2O adsorption [14]	-0.94	-1.03	-0.99
OH + H adsorption [14]	-1.34	-1.28	-1.22
OH + H adsorption [10]	N/A	N/A	-0.96
H_2O adsorption [12]	-0.87	-0.83	-0.79
OH + H adsorption [12]	-1.12	-1.12	-0.95

Table 8: Adsorption energies in eV per water molecule on PuO_2 (110).

System	CeO_2 (110) + 1 × H_2O	CeO_2 (110) + 2 × H_2O	CeO_2 (110) + 4 × H_2O
H_2O adsorption [21]	-0.85	-0.76	N/A
OH + H adsorption [21]	-1.12	-1.00	-0.21

Table 9: Adsorption energies in eV per water molecule on CeO_2 (110).

Distance (Å)	UO_2 (110) + 0.25 - 1.0 ML	PuO_2 (110) + 0.25 - 1.0 ML	CeO_2 (110) + 0.25 - 1.0 ML [21]
H_W - O_{1S}	2.13 - 2.26	2.14 - 2.21	2.07
An_S/Ce_S - H_2O	2.73	2.72	2.67
An_S/Ce_S - O_WH_W	2.15	2.12	2.14
An_S/Ce_S - O_SH_W	2.44 - 2.58	2.44 - 2.49	2.48 - 2.58
O_SH_W - O_WH_W	3.11	3.05	1.92

Table 10: Selected inter-atomic distances for molecularly and dissociatively adsorbed water on the UO_2 (110) and PuO_2 (110) surfaces at coverages from 0.25 to 1.0 mono-layers, and results for CeO_2 (110) from Molinari et al. [21]. H_W and O_W denote the hydrogen and oxygen atoms belonging to the water molecule whereas An_S/Ce_S and O_S denote the outermost surface atoms. O_WH_W denotes the hydroxyl molecule made from the dissociated water molecule and O_SH_W denotes the other hydroxyl molecule made from a surface oxygen and the remaining hydrogen.

Comparing the adsorption energies in tables 7 and 8, we find good agreement with earlier studies on UO_2 and PuO_2, with the added observation that unlike the (111) surface, there is a clear preference for dissociative adsorption at all coverages on the (110) surface, leading to the prediction that this surface should be fully hydroxylated. This trend is consistent across all previous studies, despite the slightly different equilibrium geometries found. Furthermore, we again find good agreement with ceria at all coverages.

The interatomic distances in table 10 again reveal similar hydrogen bond distances H_W - O_S for UO_2 and PuO_2, suggesting similar hydrogen bonds present. We also find similar An_S - H_2O distances, suggesting similar adsorption

geometries. Moreover, the An_S - O_WH_W distances are again comparatively shorter, again suggesting the hydroxyls sit closer to the surface than the molecular water. However, despite the O_SH_W - O_WH_W hydroxyl distances being larger than on the (111) surface, we do not see any changes with coverage on the (110) surface that would suggest weaker intra-molecular hydrogen bonding, unlike the (111) surface.

Commented [A5]: Again, "demonstrating" seems more appropriate to me.

As with (111), we now investigate mixed adsorption on the (110) surface at full coverage, going from fully molecular to fully hydroxylated. The adsorption energies are shown in tables 11 and 12. Corresponding data from Bo and colleagues [10], Rák et al. [13], Wellington and others [14], and Jomard and coworkers [12], are shown for comparison. Unlike the (111) surface, we find the fully dissociated case to be the most stable for the (110), supporting our previous predictions of a fully hydroxylated first layer [14]. Note, however, that Bo and co-workers [10] find a very slight preference for mixed adsorption on UO_2 (110), which neither we nor Wellington et al. [14], observe.

System	UO_2 (110) + 4 × H_2O	UO_2 (110) + 3 × H_2O + 1 × (OH + H)	UO_2 (110) + 2 × H_2O + 2 × (OH + H)	UO_2 (110) + 1 × H_2O + 3 × (OH + H)	UO_2 (110) + 4 × (OH + H)
This work	-0.65	N/A*	-0.84	-0.84	-1.00
Wellington *et al.* [14]	-0.90	-1.02	-1.18	-1.24	-1.34

Bo *et al.* [10]	-0.62	-0.82	-1.00	-0.98	-0.93
Rák *et al.* [13]	N/A	N/A	N/A	N/A	-1.05

Table 11: Adsorption energies in eV per water molecule on UO_2 (110) for mixed molecular and dissociative adsorption. * We were unable to converge the correct magnetic state for this configuration.

System	PuO_2 (110) + 4 × H_2O	PuO_2 (110) + 3 × H_2O + 1 × (OH + H)	PuO_2 (110) + 2 × H_2O + 2 × (OH + H)	PuO_2 (110) + 1 × H_2O + 3 × (OH + H)	PuO_2 (110) + 4 × (OH + H)
This work	-0.39	N/A*	-0.83	-0.78	-0.91
Wellington *et al.* [14]	-0.99	-1.08	-1.16	-1.13	-1.22
Rák *et al.* [13]	N/A	N/A	N/A	N/A	-0.96
Jomard *et al.* [12]	-0.79	N/A	N/A	N/A	-0.95

Table 12: Adsorption energies in eV per water molecule on PuO_2 (110) for mixed molecular and dissociative adsorption. * We were unable to converge the correct magnetic state for this configuration.

Adsorption on the AnO_2 (100) surface

The (110) surface consists of alternating layers of An and O atoms, where the surface charge depends on the termination. This forces us to move half the oxygen atoms from bottom to the top to balance the charge. We again adsorb on both surfaces to improve symmetry and avoid dipole effects. A ball-and-stick representation of a single water adsorbing on the (100) surface is shown in figure 3.

Commented [A6]: I wonder if we should illustrate this with a diagram. I can't work out what has been done when lo0oking at Figure 3.

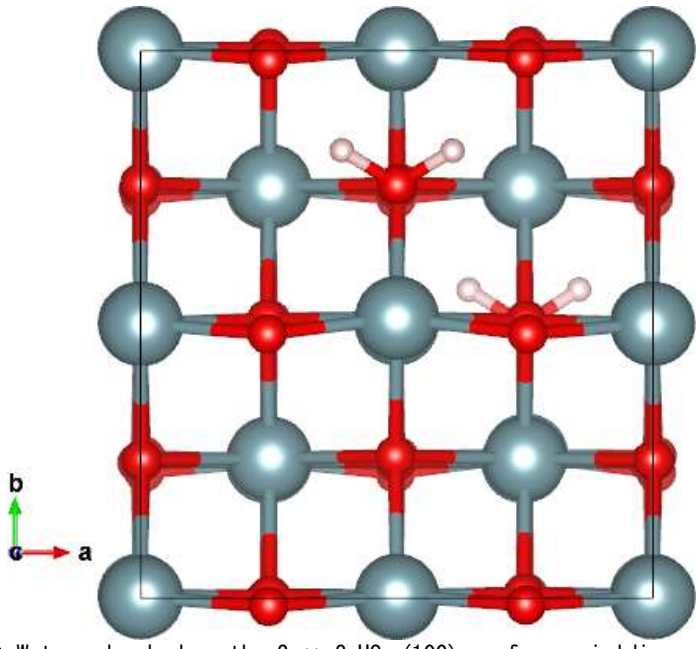

Figure 3: Water adsorbed on the 2 × 2 UO_2 (100) surface, yielding a coverage of 25%, i.e. ¼ of a mono-layer. U atoms in gray, oxygen in red and hydrogen in white. Adsorption occurs on both sides of the slab and, as the two surfaces have equivalent sites that are offset, we can see both the top and the bottom water molecules.

Calculated adsorption energies for molecularly and dissociatively adsorbed water on UO_2 (100) and PuO_2 (100) are given in tables 13 and 14. Additional data on UO_2 from Bo and co-workers [10], UO_2 and PuO_2 from Rák and colleagues [13] are again shown for comparison. Corresponding data on CeO_2 (100) from Molinari and co-workers [21] are shown in table 15 and selected inter-atomic distances are shown in table 16.

System	UO_2 (100) + 1 × H_2O	UO_2 (100) + 2 × H_2O	UO_2 (100) + 4 × H_2O
H_2O adsorption	-0.97	-0.87	-0.86
OH + H adsorption	-1.55	-1.44	-1.01
H_2O adsorption [10]	-1.02	-0.93	-0.91
OH + H adsorption [10]	-1.71	-1.55	-0.99
OH + H adsorption [13]	N/A	N/A	-1.29

Table 13: Adsorption energies in eV per water molecule on UO_2 (100).

System	PuO_2 (100) + 1 × H_2O	PuO_2 (100) + 2 × H_2O	PuO_2 (100) + 4 × H_2O
H_2O adsorption	-1.12	-1.00	-0.95
OH + H adsorption	-1.76	-1.64	-1.37
OH + H adsorption [13]	N/A	N/A	-1.46

Table 14: Adsorption energies in eV per water molecule on PuO_2 (100).

System	CeO_2 (100) + 1 × H_2O	CeO_2 (100) + 2 × H_2O	CeO_2 (100) + 4 × H_2O
H_2O adsorption [21]	-1.00	N/A	-0.89
OH + H adsorption [21]	-1.57	-1.73/-0.87	-0.89

Table 15: Adsorption energies in eV per water molecule on CeO_2 (100).

Distance (Å)	UO_2 (100) + 0.25 - 1.0 ML	PuO_2 (100) + 0.25 - 1.0 ML	CeO_2 (100) + 0.25 - 1.0 ML [21]
H_W – O_{1S}	1.75 - 1.97	1.71 - 1.92	1.97 - 2.11
An_S/Ce_S - H_2O	2.57 - 2.84	2.50 - 2.89	2.64 - 2.70
An_S/Ce_S – O_WH_W	2.26 - 2.35	2.29 - 2.34	2.34 - 2.37
An_S/Ce_S – O_SH_W	2.34 - 2.46	2.36 - 2.51	2.36 - 2.45
O_SH_W – O_WH_W	2.77 - 296	2.69 - 2.91	2.52

Table 16: Selected inter-atomic distances for molecularly and dissociatively adsorbed water on the UO_2 (100) and PuO_2 (100) surfaces at coverages from 0.25 to 1.0 mono-layers, and results for CeO_2 (100) from Molinari et al. [21]. H_W and O_W denote the hydrogen and oxygen atoms belonging to the water molecule whereas An_S/Ce_S and O_S denote the outermost surface atoms. O_WH_W denotes the hydroxyl molecule made from the dissociated water molecule and O_SH_W denotes the other hydroxyl molecule made from a surface oxygen and the remaining hydrogen.

Examining the energies in tables 13 and 14, we again find a good agreement with earlier studies on UO_2 (100). As with the (110) surface, there is a clear preference for dissociative adsorption at all coverages on the (100) surface; hence both the (110) and (100) surfaces are predicted to be fully hydroxylated. Moreover, we note that unlike the (111) and (110) surfaces, PuO_2 (100) has larger adsorption energies compared with UO_2 (100).

Inspecting the inter-atomic distances in table 16, we find comparatively shorter hydrogen bond distances H_W – O_S for the AnO_2 (100) surfaces, suggesting stronger bonds compared to the (111) and (110) surfaces. There is also a slight distortion of the surface oxygens, shortening the H_W – O_S bond. We again find similar An_S - H_2O distances for both UO_2 and PuO_2, suggesting the

Commented [A7]: This might be true, but my feeling is that we haven't ruled out a different origin here, namely that the surface isn't really that of AnO2 but of AnO(2-x) since we've redistributed the oxygens on the other surface. It doesn't therefore seem surprising that we predict dissociation to be preferable since this would partially restore the stoichiometry. It's not obvious that we can do anything about this, but I wonder if we should be more cautious in our prediction?

same type of adsorption. Moreover, the An_S - O_WH_W distances are again comparatively shorter than the An_S - H_2O distances, again suggesting the hydroxyls sit closer to the surface than the molecular water. However, despite the O_SH_W – O_WH_W hydroxyl distances again being larger than on the (111) surface, like with the (110) surface, we do not see any changes with increasing coverage on the (100) surface that would indicate weaker intra-molecular hydrogen bonding.

As before, we again investigate mixed adsorption at full coverage, going from fully molecular to fully hydroxylated. The adsorption energies are shown in tables 17 and 18 below. Corresponding data from Bo *et al.* [10] and Rák and co-workers [13]are shown for comparison. For both UO_2 and PuO_2, there is a general trend towards increased favorability of all-dissociative adsorption, although for UO_2 the most stable arrangement is a three-to-one ratio of dissociative to molecular. We attribute this to slightly stronger hydrogen bonding in this particular case, due to the presence of a shorter hydrogen bond of 1.62 Å between the adsorbed water molecule and the hydroxyls on the surface. Unlike (111) and (110), we find larger adsorption energies on PuO_2 (100) than UO_2 (100) for the more dissociative cases.

System	UO_2 (100) + 4 × H_2O	UO_2 (100) + 3 × H_2O + 1 × (OH + H)	UO_2 (100) + 2 × H_2O + 2 × (OH + H)	UO_2 (100) + 1 × H_2O + 3 × (OH + H)	UO_2 (100) + 4 × (OH + H)
This work	-0.86	-0.96	-0.95	-1.24	-1.01

Bo *et al.* [10]	-0.91	N/A	N/A	N/A	-0.99
Rák *et al.* [13]	N/A	N/A	N/A	N/A	-1.29

Table 17: Adsorption energies on UO_2 (100) in eV per water molecule for mixed molecular and dissociative adsorption.

System	PuO_2 (100) + 4 × H_2O	PuO_2 (100) + 3 × H_2O + 1 × (OH + H)	PuO_2 (100) + 2 × H_2O + 2 × (OH + H)	PuO_2 (100) + 1 × H_2O + 3 × (OH + H)	PuO_2 (100) + 4 × (OH + H)
This work	-0.95	-0.78	-1.21	-1.37	-1.37
Rák *et al.* [13]	N/A	N/A	N/A	N/A	-1.46

Table 18: Adsorption energies on PuO_2 (100) in eV per water molecule for mixed molecular and dissociative adsorption.

To summarize the adsorption data for the three target surfaces, we find that on the (111) surface there is a slight preference for a 50/50 mix of molecular and dissociative adsorption for both UO_2 and PuO_2, although the difference in adsorption energy is only 0.06 - 0.1 eV/water molecule compared with the fully molecular case. By contrast, on the (110) and (100) surfaces there is a clear preference for dissociative adsorption for both oxides, leading us to predict that both of these surfaces will be fully hydroxylated.

Desorption temperatures from the AnO_2 surfaces

We have investigated the stability of the monolayer-covered UO_2 and PuO_2 surfaces by calculating the temperature of water desorption (T_d), with the

aim of predicting the temperatures at which wet surfaces become dry for a given partial pressure of water. The desorption temperature at a given pressure is calculated from the equation below, which has been used previously for other material surfaces [21], [24], [25], [26].

$$\gamma_{s,wet,(T,p)} = \gamma_{s,dry} + \left(C \times \left(E_{ads,(T)} - RTln(p/p_0)\right)\right)$$

The surface energy of the dry surface is defined as $\gamma_{s,dry} = \left(E_{slab,dry} - E_{bulk}\right)/2S$ with $E_{slab,dry}$ the energy of the dry slab, E_{bulk} the energy of AnO_2 bulk and $\boldsymbol{S}$ the surface area. The adsorption energy per water molecule is $E_{ads,(T)} = E_{slab,wet} - \left(E_{slab,dry} + n_{H_2O} \times E_{H_2O,(T)}\right)/n_{H_2O}$ with $E_{slab,wet}$ the energy of the monolayer adsorbed slab, n_{H_2O} the number of adsorbed water molecules and $E_{H_2O,(T)} = E_{H_2O,(g)} - TS^o_{(T)}$ where $S^o_{(T)}$ is the experimental entropy of gaseous water in the standard state [27], given by $S^o_{(T)} = 1.4347^{-7}x^3 - 3.2221^{-4}x^2 + 2.8391^{-1}x + 1.2846^{-2}$. C is the coverage in mol/m^2, E_{ads} is the adsorption energy in J/mol, T is the temperature, and p and p^0 are the chosen and standard state (1 bar) partial pressures of water ~~chosen and in the standard state (1 bar)~~, respectively.

Commented [A8]: Approximated by?

In Table 19 we give the T_d data for the most stable fully covered configuration for each surface. Desorption temperatures for less stable configurations on each surface can be found in the Supplementary Information. Water is predicted to desorb from the AnO_2 (111) surfaces at temperatures between 120 - 319 K, whereas it will remain on the (110) and (100) until temperatures of

208 - 650 K depending on the vapor pressure. We find slightly lower desorption temperatures for the PuO_2 (111) and (110) surfaces than for UO_2, which is to be expected from the slightly lower adsorption energies. Moreover, we find the highest desorption temperatures for fully hydroxylated PuO_2 (100), again as expected from the higher adsorption energies found for this system. Our temperatures compare well with earlier work on CeO_2 by Molinari *et al.* [21], who found desorption temperatures of 325 K for the (111) surface, 575 K for the hydroxylated (110) surface and 825 K for the hydroxylated (100) surface, all at atmospheric pressure.

Commented [A9]: Partial pressure?

Focusing on PuO_2 at atmospheric pressure, we find desorption temperatures of 265 K for the (111) surface, 434 K for the (110) surface and 615 K for the (100) surface. As noted in the introduction, Stakebake's experiments [3] found two distinct water desorption temperature ranges, 573 - 623 K and 373 - 423 K, the former being interpreted as being due to waters bound directly to the PuO_2 surface, with the lower range due to more weakly bound second layer (or above) waters. An alternative explanation, on the basis of our calculations, is that these ranges are due to water desorbing from the most strongly bound layers on the (100) and (110) surfaces respectively. Future calculations of multiple layers of water on our target surfaces will give further insight into this suggestion.

Conf. / Pressure	UO_2 (111) + 2 × H_2O + 2 × (OH + H)	PuO_2 (111) + 2 × H_2O + 2 × (OH + H)	UO_2 (110) + 4 × (OH + H)	PuO_2 (110) + 4 × (OH + H)	UO_2 (100) + 1 × H_2O + 3 × (OH + H)	PuO_2 (100) + 4 × (OH + H)
p = 10^{-13} bar	138	120	228	208	271	302
p = 10^{-7} bar	186	162	301	276	356	396
p = 1 bar	300	265	472	434	555	615
p = 3 bar	313	277	490	452	577	638
p = 5 bar	319	282	499	460	587	650

Table 19: Calculated water desorption temperatures in K as a function of pressure for the most stable fully covered configurations on the (111), (110) and (100) surfaces of UO_2 and PuO_2.

Conclusions

In this study we have investigated water adsorption on three low index surfaces of UO_2 and PuO_2, comparing molecular and dissociative adsorption at coverages of up to one monolayer. We find a mix of molecular and dissociative adsorption to be most stable on the (111) surface, and that fully dissociative adsorption is the most stable configuration on the (110) and (100) surfaces, leading to a fully hydroxylated monolayer. This is the first time that data for all three surfaces of both target oxides have been calculated in a single study, and our results compare well with data from less complete earlier studies, allowing us to identify confidently the most stable adsorption configuration on each surface.

We have used our calculated adsorption energies to predict desorption temperatures of the most stable configurations for each oxide and surface. These suggest that water will be present as hydroxylated (110) and (100) surfaces even at elevated temperatures and pressures, conditions likely to be found in the UK's PuO_2 storage canisters. Our room temperature data for PuO_2 lead us to tentatively ascribe experimentally determined desorption temperatures to desorptions from the hydroxylated (110) and (100) surface monolayers.

We are continuing to explore water adsorption on the AnO_2 surfaces, now tackling more complex problems such as defect surfaces and multiple water layers, and will report the results of these studies in future contributions.

Acknowledgements

We would like to thank the EPSRC's "DISTINCTIVE" consortium (http://www.distictiveconsortium.org, EP/L014041/1) for funding. We also thank the University of Manchester for computing resources via the Computational Shared Facility (CSF) and for access to the "Polaris" cluster at the N8 HPC Centre of Excellence, provided and funded by the N8 consortium and EPSRC (Grant No.EP/K000225/1). The Centre is co-ordinated by the Universities of Leeds and Manchester. We also thank University College London for computing resources *via* Research Computing's "Legion" cluster (Legion@UCL) and associated services, and the "Iridis" facility of the e-Infrastructure South Consortium's Centre for Innovation. We are also grateful to the HEC Materials Chemistry Consortium, which is funded by EPSRC (EP/L000202), for access to ARCHER, the UK's National Supercomputing Service (http://www.archer.ac.uk). Finally, we thank Howard Sims and Robin Orr of the National Nuclear Laboratory, and Jeffrey Hobbs and Helen Steele at Sellafield Ltd, for helpful discussions.

References

[1] Global Fissile Materials Report 2015, http://fissilematerials.org/library/gfmr15.pdf

[2] J.M. Haschke, T.E. Ricketts, Adsorption of water on plutonium dioxide, J. Alloys Compd. 252 (1997) 148-156. doi:10.1016/S0925-8388(96)02627-8.

[3] J.L. Stakebake, Thermal desorption study of the surface interactions between water and plutonium dioxide, J. Phys. Chem. 77 (1973) 581-586. doi:10.1021/j100624a003.

[4] M. Paffett, D. Kelly, S. Joyce, J. Morris, K. Veirs, A critical examination of the thermodynamics of water adsorption on actinide oxide surfaces, J. Nucl. Mater. 322 (2003) 45–56. doi:10.1016/S0022-3115(03)00315-5.

[5] F.N. Skomurski, L.C. Shuller, R.C. Ewing, U. Becker, Corrosion of UO_2 and ThO_2: A quantum-mechanical investigation, J. Nucl. Mater. 375 (2008) 290-310. doi:10.1016/j.jnucmat.2007.12.007.

[6] P.F. Weck, E. Kim, C.F. Jové-Colón, D.C. Sassani, On the role of strong electron correlations in the surface properties and chemistry of uranium dioxide., Dalton Trans. 42 (2013) 4570-8. doi:10.1039/c3dt32536a.

[7] X-f. Tian, H. Wang, H-x. Xiao, T. Gao, Adsorption of water on UO2 (1 1 1) surface: Density functional theory calculations, Comput. Mater. Sci., 91 (2014) 364-371. doi:10.1016/j.commatsci.2014.05.009.

[8] S. L. Dudarev , D. Nguyen Manh, A. P. Sutton, Effect of Mott-

Hubbard correlations on the electronic structure and structural stability of uranium dioxide, Philos. Mag. Part B, 75, (1997) 613-628, DOI: 10.1080/13642819708202343

[9] A. I. Liechtenstein, V. I. Anisimov, J. Zaanen, Density-functional theory and strong interactions: Orbital ordering in Mott-Hubbard insulators, Phys. Rev. B. 52 (1995) R5467, doi: 10.1103/PhysRevB.52.R5467

[10] T. Bo, J.-H. Lan, Y.-L. Zhao, Y. Zhang, C.-H. He, Z.-F. Chai, et al., First-principles study of water adsorption and dissociation on the UO_2 (111), (110) and (100) surfaces, J. Nucl. Mater. 454 (2014) 446 - 454. doi:10.1016/j.jnucmat.2014.09.001.

[11] X. Wu, A. Ray, Density-functional study of water adsorption on the PuO_2 (110) surface, Phys. Rev. B. 65 (2002) 085403. doi:10.1103/PhysRevB.65.085403.

[12] G. Jomard, F. Bottin, G. Geneste, Water adsorption and dissociation on the PuO_2 (110) surface, J. Nucl. Mater. 451 (2014) 28 - 34. doi:10.1016/j.jnucmat.2014.03.012.

[13] Z. Rák, R.C. Ewing, U. Becker, Hydroxylation-induced surface stability of AnO_2 (An=U, Np, Pu) from first-principles, Surf. Sci. 608 (2013) 180-187. doi:10.1016/j.susc.2012.10.002.

[14] J. P. W. Wellington, A. Kerridge, J. Austin, N. Kaltsoyannis, J. Nucl. Mat. (2016) doi:10.1016/j.jnucmat.2016.10.005.

[15] G. Kresse, J. Hafner, Ab initio molecular dynamics for liquid metals,

Phys. Rev. B. 47 (1993) R558, doi: 10.1103/PhysRevB.47.558

G. Kresse, J. Hafner, Ab initio molecular-dynamics simulation of the liquid-metal-amorphous-semiconductor transition in germanium, Phys. Rev. B. 49 (1994) 14251, doi: 10.1103/PhysRevB.49.14251

G. Kresse, J. Furthmüller, Efficiency of ab-initio total energy calculations for metals and semiconductors using a plane-wave basis set, Comput. Mater. Sci., 6 (1996) 15-50, doi: 10.1016/0927-0256(96)00008-0

G. Kresse, J. Furthmüller, Efficient iterative schemes for ab initio total-energy calculations using a plane-wave basis set, Phys. Rev. B. 54 (1996) 11169, doi: 10.1103/PhysRevB.54.11169

[16] P. E. Blöchl, Projector augmented-wave method, Phys. Rev. B. 50 (1994) 17953, doi: 10.1103/PhysRevB.50.17953

G. Kresse, D. Joubert, From ultrasoft pseudopotentials to the projector augmented-wave method, Phys. Rev. B. 59 (1999) 1758, doi: 10.1103/PhysRevB.59.1758

[17] H. J. Monkhorst, J. D. Pack, Special points for Brillouin-zone integrations, Phys. Rev. B. 13 (1976) 5188, doi: 10.1103/PhysRevB.13.5188

[18] J.P. Perdew, K. Burke, M. Ernzerhof, Generalized Gradient Approximation Made Simple [Phys. Rev. Lett. 77, 3865 (1996)], Phys. Rev. Lett. 78 (1997) 1396-1396. doi:10.1103/PhysRevLett.78.1396.

[19] J. Schoenes, Optical properties and electronic structure of UO_2, J. Appl.

Phys. 49 (1978) 1463. doi:10.1063/1.324978.

[20] T.M. McCleskey, E. Bauer, Q. Jia, A.K. Burrell, B.L. Scott, S.D. Conradson, et al., Optical band gap of NpO_2 and PuO_2 from optical absorbance of epitaxial films, J. Appl. Phys. 113 (2013) 013515. doi:10.1063/1.4772595.

[21] M. Molinari, S. C. Parker, D. C. Sayle, M. S. Islam, Water Adsorption and Its Effect on the Stability of Low Index Stoichiometric and Reduced Surfaces of Ceria, J. Phys. Chem. C 116 (2012), 7073-7082, doi: 10.1021/jp300576b

[22] F. Bottin, G. Geneste, G. Jomard, Thermodynamic stability of the UO2 surfaces: Interplay between over-stoichiometry and polarity compensation, Phys. Rev. B. 93 (2016) 115438 doi: 10.1103/PhysRevB.93.115438

[23] I.D. Prodan, G.E. Scuseria, R.L. Martin, Assessment of metageneralized gradient approximation and screened Coulomb hybrid density functionals on bulk actinide oxides, Phys. Rev. B - Condens. Matter Mater. Phys. 73 (2006) 1-10. doi:10.1103/PhysRevB.73.045104.

[24] C. Arrouvel, M. Digne, M. Breysse, H. Toulhoat, P. Raybaud, Effects of morphology on surface hydroxyl concentration: a DFT comparison of anatase-TiO2 and γ-alumina catalytic supports, J. Catal., 222 (2004), 152-166, doi: 10.1016/j.jcat.2003.10.016.

[25] Q. Sun, K. Reuter, M. Scheffler, Effect of a humid environment on the surface structure of RuO2(110), Phys. Rev. B.67 (2003) 205424, doi:

10.1103/PhysRevB.67.205424

[26] S. Kerisit, A. Marmier, S. C. Parker, Ab Initio Surface Phase Diagram of the {1014} Calcite Surface, J. Phys. Chem. B 109 (2005), 18211-18213, doi: 10.1021/jp053489x

[27] Data from http://kinetics.nist.gov/janaf/html/H-064.html